

dependent on structural features, such as ring size, ring substitution, or ring unsaturation.

With the rate constants from the linear approximation of $k_{\text{obsd}}/[\text{H}^+]$ at low $[\text{H}^+]$ for comparison, the rate constant decreases from $6 \times 10^{-4} \text{ L mol}^{-1} \text{ s}^{-1}$ for $[\text{Ni}(\text{trans}-[18]\text{diene})]^{2+}$ to $9.6 \times 10^{-6} \text{ L mol}^{-1} \text{ s}^{-1}$ for $[\text{Ni}(\text{trans}-[15]\text{diene})]^{2+}$. The reaction for $[\text{Ni}(\text{trans}-[16]\text{diene})]^{2+}$ is kinetically more complex, but the rate is between those of the [18] and [15] homologues.³⁸ Reaction of $[\text{Ni}(\text{trans}-[14]\text{diene})]^{2+}$ with acid is extremely slow, with a rate constant in 2 mol L⁻¹ HCl at 25 °C of ca. 10^{-9} s^{-1} .³⁸ Preliminary studies on the 13-membered monoimine complex $[\text{Ni}(\text{[13]ene})]^{2+}$ ³⁸ show hydrolysis rates comparable to those of $[\text{Ni}(\text{trans}-[15]\text{diene})]^{2+}$, confirming that the rate minimum occurs for the 14-membered macrocycles.

For the copper(II) compounds the comparison is complicated by the change in kinetic form. However, for the trans macrocycles the rate decreases from the [18] to the [16] species (acid-limiting kinetics), and for the cis macrocycles the rate decreases from the [15] to the [14] species (and then increases for $[\text{Cu}(\text{[13]ene})]^{2+}$),³⁸ all with second order dependence on $[\text{H}^+]$. As for the nickel(II) analogues, available evidence indicates that the hydrolysis rate is a minimum for the 14-membered tetraaza macrocycle cations.

Although metal ion compounds of noncyclic imine ligands are usually very readily hydrolyzed, the compounds of the macrocyclic diimines in this study are clearly very resistant to acid hydrolysis. Studies reported in 6.1 mol L⁻¹ HCl showed that $[\text{Cu}(\text{trans}-[14]\text{diene})]^{2+}$ reacted more rapidly than the compound of the *C-meso* tetraamine formed by reduction of the imine functions.²² However, measurements at a single acid concentration can be misleading, since the diimine compound shows second-order dependence of rate on $[\text{H}^+]$, while metastable nitrogen isomers of the tetraamine compounds show consecutive reactions with first-order dependence of rate on $[\text{H}^+]$.⁸ Studies in progress indicate that the stable isomer of the *C-meso* tetraamine complex reacts more slowly than $[\text{Cu}(\text{trans}-[14]\text{diene})]^{2+}$, and the rate constants show second-order dependence on $[\text{H}^+]$.³⁸ The nickel(II) compounds of cyclic tetraamines formed by reduction of the imine

functions of *trans*-[16]diene, *trans*-[15]diene, and Me[15]diene all react with acid considerably more rapidly than do their diimine analogues³⁸ (in line with rates published for the unsubstituted cyclic amines).¹⁸ The presence of rigid imine groups makes the macrocycles much less flexible and could thus make conformational changes associated with movement of a dissociated nitrogen away from the coordination site more difficult. Once freed from coordination, the imine function would be subject to relatively rapid acid hydrolysis, opening the macrocycle. The reaction thereafter should proceed at rates similar to those of compounds of noncyclic polyamines. The kinetic results for the hydrolysis of the copper(II) compounds that show second-order dependence on $[\text{H}^+]$ suggest that the breaking of the second (or third, in the alternative kinetic interpretation, discussed above) copper-nitrogen bond may be rate-determining. This would indicate that the first (or first two) bonds dissociated are to secondary amine groups.

For copper(II) the cis diene macrocycle compounds react more rapidly than their trans isomer, by a factor of 10 for the [14] pair, with a much greater difference for the [18] pair.⁸ For nickel(II) the cis isomer for the [15] pair reacts more rapidly by a factor of 1.7, while for the [14] system the cis isomer reacts even more slowly than the trans isomer.³⁸

Increased C- or N-substitution of amine ligands generally reduces the rate of reaction with acid of their metal ion complexes.³ This effect is shown for $[\text{Ni}(\text{trans}-[15]\text{diene})]^{2+}$ and $[\text{Ni}(\text{Me}-[15]\text{diene})]^{2+}$, where the additional axially oriented methyl group, added to an already crowded coordination environment, reduces the rate by 1 order of magnitude. This effect must be stereochemical in origin and is understandable if a conformational change of the macrocycle is important in determining the rate of the slow dissociation step.

Acknowledgment. The financial assistance of the Research Committee of the New Zealand Universities Grants Committee is gratefully acknowledged.

Registry No. $[\text{Cu}(\text{trans}-[14]\text{diene})]^{2+}$, 33727-13-8; $[\text{Ni}(\text{trans}-[15]\text{diene})]^{2+}$, 47180-49-4; $[\text{Ni}(\text{trans-Me}[15]\text{diene})]^{2+}$, 93251-62-8; $[\text{Cu}(\text{trans}-[16]\text{diene})]^{2+}$, 67551-52-4; $[\text{Cu}(\text{cis}-[14]\text{diene})]^{2+}$, 34679-83-9; $[\text{Cu}(\text{cis}-[15]\text{diene})]^{2+}$, 47180-28-9; $[\text{Ni}(\text{cis}-[15]\text{diene})]^{2+}$, 47180-29-0.

(38) Curtis, N. F., unpublished observations.

Contribution from the Department of Inorganic Chemistry,
The University, Newcastle upon Tyne NE1 7RU, U.K.

Kinetics of the Substitution of Thiocyanate and Oxalate on $[\text{Mo}_3\text{O}_4(\text{H}_2\text{O})_9]^{4+}$: High Acidity of the Aqua Ligands and the Dominance of Conjugate-Base Pathways

Bee-Lean Ooi and A. Geoffrey Sykes*

Received May 27, 1987

The influence of $[\text{H}^+]$ on substitution reactions of $[\text{Mo}_3\text{O}_4(\text{H}_2\text{O})_9]^{4+}$ is addressed. From the kinetic treatment given, the trimer has an exceptionally high acid dissociation constant $K_{\text{aM}}(25 \text{ }^\circ\text{C})$ of 0.42 M (average), $I = 2.00 \text{ M}$ (LiPTS), and as far as can be ascertained substitution with NCS^- and HC_2O_4^- proceeds solely by the trimer conjugate-base form. Rate constants for NCS^- ($4.8 \text{ M}^{-1} \text{ s}^{-1}$) and HC_2O_4^- ($3.3 \text{ M}^{-1} \text{ s}^{-1}$) reacting with the conjugate base are in close agreement, consistent with an I_4 process. Substitution is believed to be at the more labile d- H_2O positions (two to each Mo) trans to the μ_2 -oxo's and is influenced by conjugate-base formation at a coordinated H_2O . Aquation steps, and chelation of monodentate HC_2O_4^- to give oxalate chelated at two d- H_2O positions, also proceed by conjugate-base pathways. The two stages involving oxalate coordination provide a further (rare) example of two reaction stages becoming interposed.

Introduction

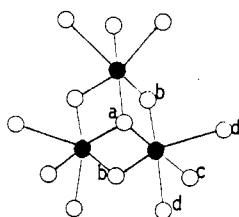
Cotton and colleagues demonstrated for the first time in 1978 the occurrence of the trimeric Mo(IV) core in a crystal study on the complex $\text{Cs}_2[\text{Mo}_3\text{O}_4(\text{C}_2\text{O}_4)_3(\text{H}_2\text{O})_3] \cdot 4\text{H}_2\text{O} \cdot 0.5\text{H}_2\text{C}_2\text{O}_4$.¹ Other crystal studies have been reported since then,²⁻⁵ and it is

now established that the metal-metal-bonded $\text{Mo}_3\text{O}_4^{4+}$ (incomplete cuboidal) cluster is the sole species relevant to the aqueous solution chemistry.⁶ Using ¹⁸O-labeling techniques, Murmann and co-workers have demonstrated that the same $\text{Mo}_3\text{O}_4^{4+}$ core is retained in the aqua ion $[\text{Mo}_3\text{O}_4(\text{H}_2\text{O})_9]^{4+}$.⁷ The latter has

(1) Bino, A.; Cotton, F. A.; Dori, Z. *J. Am. Chem. Soc.* **1978**, *100*, 5252.
(2) Bino, A.; Cotton, F. A.; Dori, Z. *J. Am. Chem. Soc.* **1979**, *101*, 3842.
(3) Schlemper, E. O.; Hussain, M. S.; Murmann, R. K. *Cryst. Struct. Commun.* **1982**, *11*, 89.

(4) Rogers, R. K.; Murmann, R. K.; Schlemper, E. O.; Shelton, M. E. *Inorg. Chem.* **1985**, *24*, 1313.
(5) Gheller, S. F.; Hambley, T. W.; Brownlee, R. T. C.; O'Connor, M. J.; Snow, M. R.; Wedd, A. G. *J. Am. Chem. Soc.* **1983**, *105*, 1527.
(6) Richens, D. T.; Sykes, A. G. *Comments Inorg. Chem.* **1981**, *1*, 141.

four different types of coordinated O atom, a to d as illustrated.



The core O atoms, consisting of one μ_3 -oxo and three μ_2 -oxo ligands, are extremely inert to substitution. Of the three H_2O 's coordinated to each Mo(IV), exchange of the two that are trans to the μ_2 -oxo ligands ($t_{1/2} \sim 20$ min at 0°C) is faster than exchange of that trans to the μ_3 -oxo ligand ($t_{1/2} = 1.1$ h at 25°C) at $[\text{H}^+] = 1.0$ M.⁴⁻⁷ From X-ray crystallography it can be concluded that the d- H_2O 's trans to the μ_2 -oxo's are less tightly bound (Mo-O distance 2.26 Å in $[\text{Mo}_3\text{O}_4(\text{NCS})_8(\text{H}_2\text{O})]^{4+}$),³ than the c- H_2O 's trans to the μ_3 -oxo ligands (Mo-O distance 2.16 Å in $[\text{Mo}_3\text{O}_4(\text{C}_2\text{O}_4)_3(\text{H}_2\text{O})_3]^{2-}$).¹

Whereas structural features are now well documented, other aspects of solution chemistry including the reactivity are less well understood. In this paper substitution properties of the aqua ion are considered with both NCS^- and oxalate as incoming ligands. Substitution of H_2O by NCS^- at a d position, and the involvement of a statistical factor,⁸⁻¹⁰ has been the subject of a previous study.¹¹ The inclusion of oxalate is appropriate since from crystallography it has been demonstrated that $\text{C}_2\text{O}_4^{2-}$ chelates at the two d positions on each Mo(IV).¹⁴ The extent of the acid dissociation of the H_2O 's in $[\text{Mo}_3\text{O}_4(\text{H}_2\text{O})_9]^{4+}$ has not yet been established, and is of prime concern in the present work. In an earlier study¹² it was noted that upon adjustment of the $[\text{H}^+]$ in the range 0.02–0.20 M, $I = 2.00$ M (LiClO_4), absorbance changes at 250 nm were not always rapidly established and that deprotonation/protonation alone is unlikely to provide a full explanation of the changes observed. Absorbance changes are small; for example, a 6% change ($t_{1/2} \sim 3$ min) was observed on adjusting the $[\text{H}^+]$ from 0.65 to 0.055 M.¹² Over short time intervals at least, the changes were reported to be reversible. As a result of these observations the $[\text{H}^+]$ in previous kinetic studies was restricted to >0.75 M (substitution)^{11,12} and >0.60 M (redox).¹³ For the oxalate complex Murmann and colleagues⁴ have given a rough estimate of the acid dissociation constant for the c- H_2O , which is trans to the μ_3 -oxo, as $K_a \sim 10^{-4}$ M. This H_2O is expected to be more acidic than the d- H_2O 's of the aqua ion, for which they estimated $K_a \sim 10^{-6}$ M. In the present work, by extending the range of $[\text{H}^+]$ for kinetic studies down to 0.20 M, it has been possible to demonstrate that acid dissociation is much more extensive, $\text{p}K_a$ between 0 and 1, in keeping with our earlier report.¹²

Experimental Section

Reagents. Sodium thiocyanate (AnalaR BDH) was recrystallized once from ethanol. Sodium molybdate, $\text{Na}_2[\text{MoO}_4] \cdot 2\text{H}_2\text{O}$ (AnalaR, BDH), oxalic acid (AnalaR, BDH), and *p*-toluenesulfonic acid, HPTS (Sigma Chemicals), were used without further purification. The lithium salt of HPTS, LiPTS, was prepared by neutralization of 4 M HPTS with lithium carbonate (reagent grade, BDH), followed by recrystallization two or three times from water. Zinc shot (AnalaR, BDH) was washed with 5 M HCl (AnalaR, BDH) and amalgamated with a 1% solution of mercuric nitrate (AnalaR, BDH).

Standardization of Reactants. Thiocyanate solutions were standardized by titration against silver(I) (Convol, BDH) with iron(III) as in-

Table I. First-Order Equilibration Rate Constants k_{eq} (25°C) for the Reaction of $\text{Mo}_3\text{O}_4^{4+}$ ($\sim 4.0 \times 10^{-5}$ M) with NCS^- , $I = 2.00$ M (LiPTS)

$[\text{H}^+]$, M	$10^3[\text{NCS}^-]$, M	10^3k_{eq} , s^{-1}	$[\text{H}^+]$, M	$10^3[\text{NCS}^-]$, M	10^3k_{eq} , s^{-1}
0.20	1.20	11.2	0.60	0.10	5.0 ^a
	1.95	11.9		1.20	4.6
	2.70	12.8		1.95	5.0
	3.50	13.8		2.70	5.6
	1.20	9.5		3.50	5.9
0.25	1.95	10.4	1.00	1.20	3.6
	2.70	11.2		1.95	4.0
	3.50	11.9		3.00	4.5
	1.20	8.6		3.50	4.7
0.30	1.95	9.2	2.00	0.10	3.9 ^b
	2.70	10.0		1.20	3.1
	3.50	10.8		2.10	3.5
	1.20	6.4		3.30	4.0
0.40	1.80	6.8	2.00	1.20	1.8
	2.25	7.1		1.50	1.9
	2.70	7.3		1.95	2.1
	3.30	8.0		2.55	2.2
				3.50	2.5

^a $[\text{Mo}_3\text{O}_4^{4+}] = 0.55 \times 10^{-3}$ M. ^b $[\text{Mo}_3\text{O}_4^{4+}] = 0.90 \times 10^{-3}$ M.

indicator. Solutions of oxalic acid and HPTS were titrated against sodium hydroxide (Convol, BDH) with phenolphthalein as indicator. The $[\text{H}^+]$'s of stock $\text{Mo}_3\text{O}_4^{4+}$ solutions, and solutions of LiPTS, were standardized by ion exchange onto Amberlite IR(H)120 resin and titration of the H^+ released. Concentrations of $\text{Mo}_3\text{O}_4^{4+}$ solutions were determined spectrophotometrically (peak at 505 nm, $\epsilon = 189$ M⁻¹ cm⁻¹/mol of trimer at 25°C). We have noted a 5% decrease in ϵ values on increasing the temperature from 10 to 35°C at $[\text{H}^+] = 2.0$ M.

Preparation of $\text{Mo}_3\text{O}_4^{4+}$. Solutions of $\text{Mo}_3\text{O}_4^{4+}$ were obtained by the method described by Cotton et al.¹⁴ involving reaction of stoichiometric amounts of Mo^{III} dimer, from the Zn/Hg reduction of Mo(VI), with sodium molybdate(VI). Portions (~ 100 cm³) of the red solution obtained ($\sim 3 \times 10^{-3}$ M) were diluted 3–4 times with 1 M HPTS and left to stand under N_2 at room temperature for at least 2 days to allow aquation of coordinated chloride. The aqua ion was purified by dilution to $[\text{H}^+] \sim 0.5$ M and loading onto a Dowex 50W-X2 cation-exchange column (20 cm \times 1.5 cm diameter). The column was washed with 0.5 M HPTS (~ 250 cm³) to remove any Mo_2^{4+} , and the $\text{Mo}_3\text{O}_4^{4+}$ was eluted as a single red band with 2.0 M HPTS. Solutions of $\text{Mo}_3\text{O}_4^{4+}$ in PTS⁻ were used in this study. Differences in the behavior of PTS⁻ and ClO_4^- solutions have been indicated previously.¹¹

Kinetic Studies. Runs were on a time scale $t_{1/2} > 1$ min and were monitored at 370 nm (NCS^-) and 360 nm (oxalate) by conventional spectrophotometry on a Perkin-Elmer Lambda 9. In both studies the NCS^- and oxalate were in large (mole) excess (>10 -fold), and the data were treated with the assumption that statistical kinetics apply, as previously demonstrated in the case of NCS^- (i.e., rate constants obtained with $[\text{NCS}^-]$ in large excess are one-third those with $[\text{Mo}_3\text{O}_4^{4+}]$ in large excess, and to allow for this difference $[\text{NCS}^-]$ values are divided by 3). Values of $[\text{NCS}^-]$ were in a range appropriate for 1:1 complex formation as the dominant process at any one Mo(IV) atom. Even so, there were small subsequent absorbance changes (most likely due to bis complex formation at a single Mo), leading to uncertainty in absorbance A_∞ values, and the Guggenheim method¹⁵ was therefore used (over 3–4 half-lives) to evaluate first-order equilibration rate constants. A single stage only was observed with NCS^- . In the case of oxalate absorbance A_∞ values were stable, but plots of $\ln(A_\infty - A_t)$ against time indicated two stages. The slopes of the linear section gave first-order equilibration rate constants k_{eq} . The equilibration rate constants for the faster process, corresponding to the chelation step (first-order equilibration rate constant k_{chel}), were estimated by using a standard consecutive treatment as for $\text{A} \rightarrow \text{B} \rightarrow \text{C}$ (rather than $\text{A} \rightleftharpoons \text{B} \rightleftharpoons \text{C}$).¹⁵ The small absorbance changes (<0.1), coupled with the nonrigorous treatment employed, make a detailed consideration of k_{chel} inappropriate. Of considerable interest is the observation of chelation as the first kinetic process in $\ln(A_\infty - A_t)$ plots (see Figure 4). The point has been made previously that for consecutive reactions, when concentrations are expressed as the sum of two exponentials, the order of the reaction steps is not specified.

- (7) Hinck, G. D.; Wyroff, D. E.; Murmann, R. K. *Polyhedron* **1986**, *5*, 487.
- (8) Buckingham, D. A.; Frances, D. J.; Sargeson, A. M. *Inorg. Chem.* **1974**, *13*, 2630.
- (9) Pohl, M. C.; Espenson, J. H. *Inorg. Chem.* **1980**, *19*, 235. Marty, W.; Espenson, J. H. *Inorg. Chem.* **1979**, *18*, 1246.
- (10) Armstrong, F. A.; Henderson, R. A.; Sykes, A. G. *J. Am. Chem. Soc.* **1980**, *102*, 6545.
- (11) Kathirgamanathan, P.; Soares, A. B.; Richens, D. T.; Sykes, A. G. *Inorg. Chem.* **1985**, *24*, 2950.
- (12) Ojo, J. F.; Sasaki, Y.; Taylor, R. S.; Sykes, A. G. *Inorg. Chem.* **1976**, *15*, 1006.
- (13) Harmer, M. A.; Richens, D. T.; Soares, A. B.; Thornton, A. T.; Sykes, A. G. *Inorg. Chem.* **1981**, *20*, 4155.

- (14) Cotton, F. A.; Marler, D. O.; Schwotzer, W. *Inorg. Chem.* **1984**, *23*, 3671.
- (15) Frost, A. A.; Pearson, R. G. *Kinetics and Mechanism*, 2nd ed.; Wiley: New York, 1961; pp 162, 49.

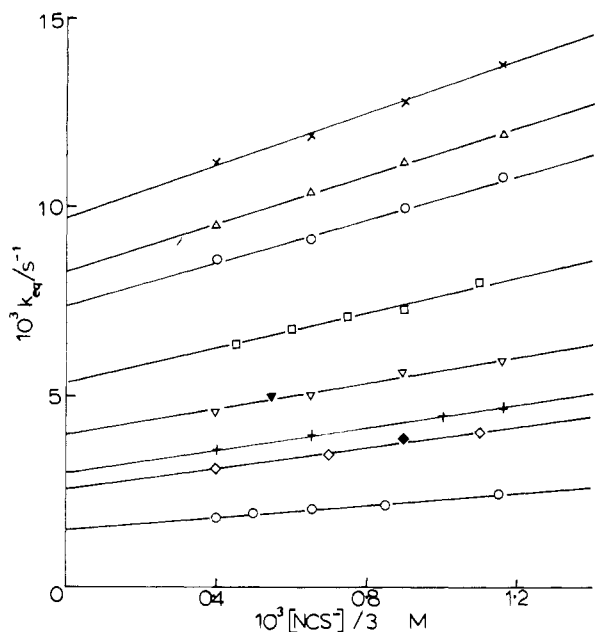


Figure 1. Dependence of first-order rate constants, k_{eq} (25 °C), for the equilibration of $\text{Mo}_3\text{O}_4^{4+}$ and NCS^- (reactant in large excess) on $[\text{NCS}^-]$ at $[\text{H}^+]/\text{M} = 0.20$ (x), 0.25 (Δ), 0.30 (O), 0.40 (□), 0.60 (▽), 0.80 (+), 1.00 (◇), 2.00 (○); $I = 2.00$ M (LiPTS). Points with $\text{Mo}_3\text{O}_4^{4+}$ in excess are indicated by solid symbols, the x-axis scale corresponding to $[\text{Mo}_3\text{O}_4^{4+}]$.

Table II. Formation (k_f) and Aquation (k_{aq}) rate constants (25 °C) for the equilibration of $\text{Mo}_3\text{O}_4^{4+}$ with NCS^- Corresponding to the Slope and Intercept, Respectively, in Figure 1, $I = 2.00$ M (LiPTS)

$[\text{H}^+]$, M	k_f , $\text{M}^{-1} \text{s}^{-1}$	$10^3 k_{aq}$, s^{-1}	$[\text{H}^+]$, M	k_f , $\text{M}^{-1} \text{s}^{-1}$	$10^3 k_{aq}$, s^{-1}
0.20	3.44 (± 0.17)	9.8 (± 0.1)	0.60	1.71 (± 0.16)	4.0 (± 0.1)
0.25	3.16 (± 0.15)	8.3 (± 0.1)	0.80	1.52 (± 0.05)	2.98 (± 0.04)
0.30	2.89 (± 0.05)	7.4 (± 0.1)	1.00	1.36 (± 0.17)	2.57 (± 0.14)
0.40	2.33 (± 0.16)	5.3 (± 0.1)	2.00	0.80 (± 0.06)	1.51 (± 0.05)

The temperature of all runs was 25.0 ± 0.1 °C. Ionic strengths were adjusted to 2.00 ± 0.01 M by using HPTS and LiPTS as required.

Treatment of Data. Unweighted linear-least-squares fits were carried out.

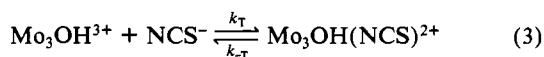
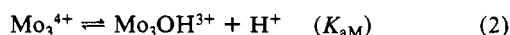
Results

Reaction with NCS^- . The dependence of first-order equilibration rate constants k_{eq} (Table I) on $[\text{NCS}^-]$ was investigated at $[\text{H}^+]$ values in the range 0.20–2.00 M. From Figure 1, k_{eq} can be expressed as in (1), which incorporates the statistical factor of

$$k_{eq} = k_f[\text{NCS}^-]/3 + k_{aq} \quad (1)$$

3,¹¹ with rate constants corresponding to 1:1 complexing of NCS^- with the trimer. Values of k_f and k_{aq} for formation and aquation steps involving $\text{Mo}_3\text{O}_4^{4+}$ and $\text{Mo}_3\text{O}_4\text{NCS}^{3+}$, respectively, are listed in Table II.

A graph of k_f against $[\text{H}^+]^{-1}$ is curved (Figure 2). The reaction scheme (2)–(4), with aqua $\text{Mo}_3\text{O}_4^{4+}$ written as Mo_3^{4+} , gives a



satisfactory fit to the data. Thus with a significant amount of the total $\text{Mo}_3\text{O}_4^{4+}$ present as the conjugate base $\text{Mo}_3\text{OH}^{3+}$, (2), the formation rate constant can be expressed as in (5). A plot

$$k_f = \frac{k_T K_{aM}}{[\text{H}^+] + K_{aM}} \quad (5)$$

of k_f^{-1} against $[\text{H}^+]$ is linear (inset to Figure 2). From a least-

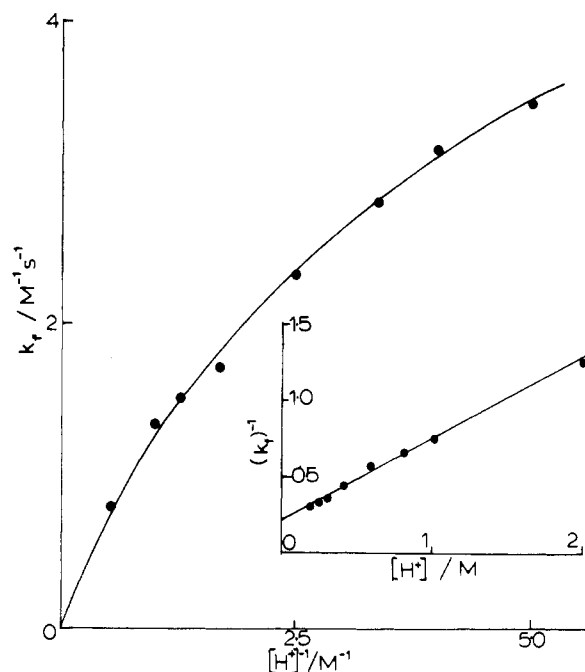


Figure 2. Variation of k_f (25 °C), for the $\text{Mo}_3\text{O}_4^{4+}$ and NCS^- complex formation step, with $[\text{H}^+]^{-1}$ at $I = 2.00$ M (LiPTS) and (inset) linear dependence of $1/k_f$ on $[\text{H}^+]$.

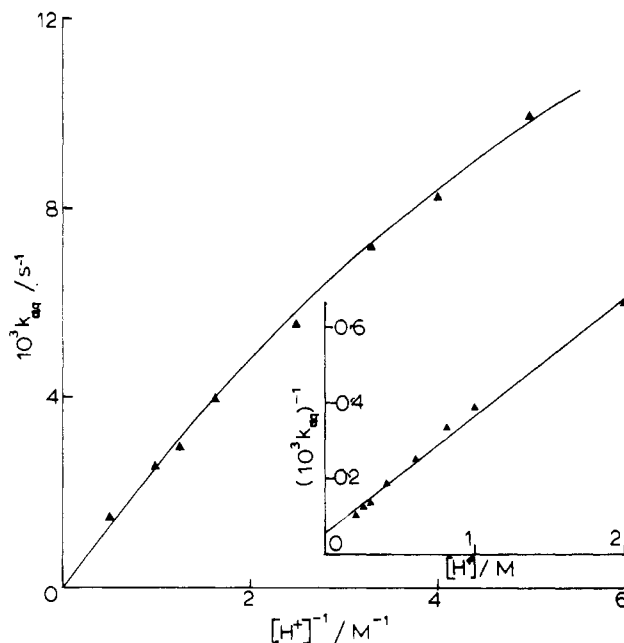


Figure 3. Variation of k_{aq} (25 °C), for the aquation of the $\text{Mo}_3\text{O}_4^{4+}$ and NCS^- complex, with $[\text{H}^+]^{-1}$ at $I = 2.00$ M [LiPTS] and (inset) linear dependence of $1/k_{aq}$ on $[\text{H}^+]$.

squares fit $k_T = 4.8 \pm 0.4 \text{ M}^{-1} \text{ s}^{-1}$ and $K_{aM} = 0.39 \pm 0.05$ M. A graph of $k_f([\text{H}^+] + K_{aM})$ against $[\text{H}^+]$ gives as best fit a horizontal line, and there is no evidence for a step involving reaction of Mo_3^{4+} with NCS^- . As far as we can tell, therefore, all of the reaction proceeds via the conjugate-base form.

Similarly, a plot of k_{aq} against $[\text{H}^+]^{-1}$ is curved (Figure 3). The expression (6) can be derived from (3) and (4). A plot of k_{aq}^{-1}

$$k_{aq} = \frac{k_T K_{aMT}}{[\text{H}^+] + K_{aMT}} \quad (6)$$

against $[\text{H}^+]$ is linear (inset to Figure 3), with $k_T = (1.72 \pm 0.30) \times 10^{-2} \text{ s}^{-1}$ and $K_{aMT} = 0.19 \pm 0.04$ M.

Runs at $[\text{H}^+] = 0.20$ and 0.25 M, with $\text{Mo}_3\text{O}_4^{4+}$ as the reactant in excess, gave rate constants higher (8–10%) than those required to fit the linear plots in Figure 1. At the higher $[\text{Mo}_3\text{O}_4^{4+}]$

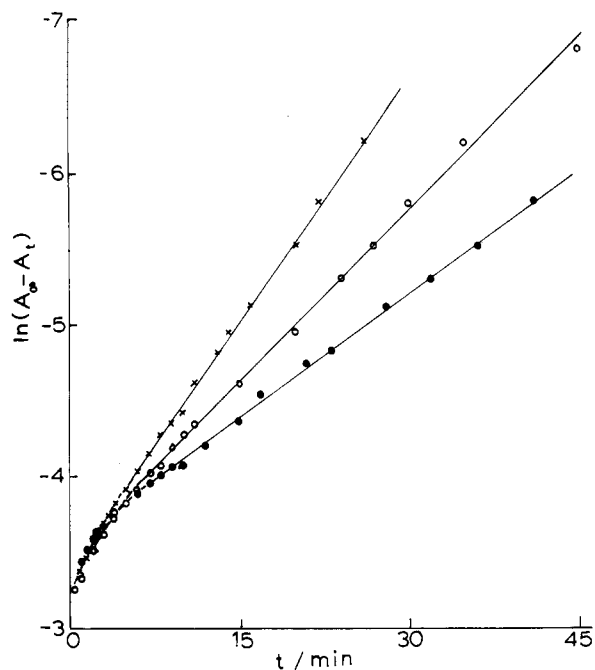


Figure 4. Representative plots of $\ln(A_\infty - A_t)$ against time at $\lambda = 360$ nm for the equilibration (25 °C) of $\text{Mo}_3\text{O}_4^{4+}$ with oxalate (reactant in large excess), $I = 2.0$ M (LiPTS), identifying two stages for the reaction.

Table III. First-Order Equilibration Rate Constants, k'_{eq} (25 °C), for the Reaction of $\text{Mo}_3\text{O}_4^{4+}$ ($\sim 1 \times 10^{-4}$ M) with Total Oxalate, $I = 2.00$ M (LiPTS), and k_{chel} , an Estimate of the Equilibration Rate Constants for the Chelation Step

$[\text{H}^+]$, M	$10^3[\text{Ox}]_T$, M	$10^3 k'_{\text{eq}}$, s^{-1}	$10^2 k_{\text{chel}}$, s^{-1}
0.2	3.3	0.90	1.11
	4.2	1.16	0.98
	5.0	1.27	1.02
	6.0	1.55	1.12
	7.2	1.76	0.95
0.3	3.0	0.66	0.60
	4.5	0.89	0.67
	5.5	1.05	0.78
	6.3	1.10	0.70
	7.0	1.26	0.61
0.5	4.0	0.74	0.60
	5.4	0.85	0.63
	6.0	0.91	0.63
	6.6	0.94	0.67
0.7	3.0	0.69	0.59
	5.0	0.79	0.61
	7.5	0.89	0.61
0.9	3.0	0.73	0.50
	5.0	0.76	0.54
	6.3	0.83	0.51
	6.6	0.85	0.51
	6.6	0.85	0.51
	7.5	0.85	0.50

required for such runs ($\sim 0.5 \times 10^{-3}$ M; cf. 0.04×10^{-3} M for runs with NCS^- in excess), and lower $[\text{H}^+]$, oligomerization of some kind is possibly incident.

Reaction with Oxalate. In contrast to the NCS^- study, plots of $\ln(A_\infty - A_t)$ against time indicate two stages for reaction with oxalate (Figure 4). From plots at constant $[\text{H}^+]$, as in Figure 4, the first kinetic stage is seen to be independent of total oxalate concentration and is therefore assigned to the chelation step. Other examples of reactions in which the two stages of reaction have in effect become interposed have been reported.¹⁶ First-order equilibration constants k'_{eq} from the linear portion of plots as in Figure 5 are listed in Table III. Estimates of equilibration rate constants for the chelation step, k_{chel} , are also given in Table III.

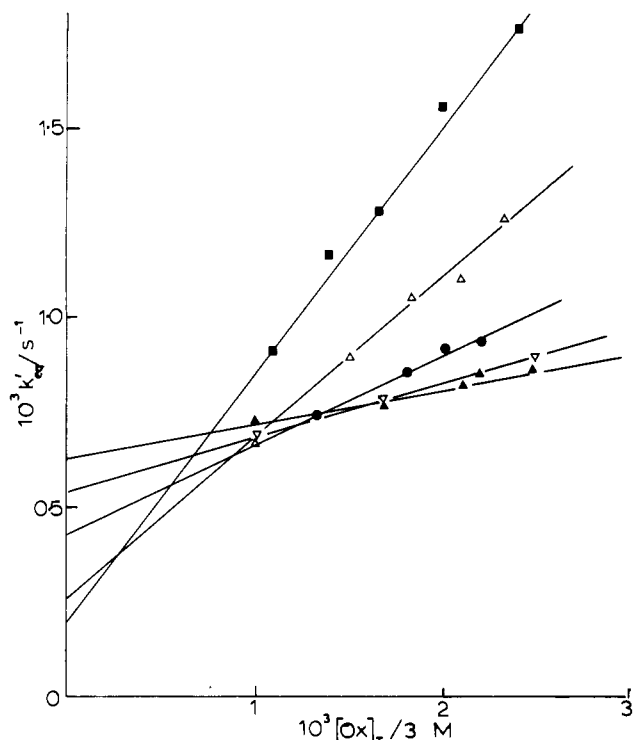


Figure 5. Dependence of first-order rate constants, k'_{eq} (25 °C), for the equilibration of $\text{Mo}_3\text{O}_4^{4+}$ and oxalate (reactant in large excess), on total oxalate at $[\text{H}^+]/M = 0.20$ (■), 0.30 (△), 0.50 (●), 0.70 (▽), 0.90 (▲); $I = 2.00$ M (LiPTS).

Table IV. Formation (k'_f) and Aquation (k'_{aq}) Rate Constants (25 °C) for the Equilibration of $\text{Mo}_3\text{O}_4^{4+}$ with Oxalate, Corresponding to the Slope and Intercept, Respectively, in Figure 5, $I = 2.00$ M (LiPTS)

$[\text{H}^+]$, M	k'_f , $\text{M}^{-1} \text{s}^{-1}$	$10^3 k'_{\text{aq}}$, s^{-1}
0.20	$0.66 (\pm 0.04)$	$0.20 (\pm 0.07)$
0.30	$0.43 (\pm 0.06)$	$0.26 (\pm 0.06)$
0.50	$0.236 (\pm 0.022)$	$0.43 (\pm 0.04)$
0.70	$0.144 (\pm 0.010)$	$0.54 (\pm 0.02)$
0.90	$0.091 (\pm 0.016)$	$0.63 (\pm 0.03)$

As in the case of the NCS^- study, the dependence on total oxalate $[\text{Ox}]_T$ (Figure 5) is of the form (7). Absorbance changes

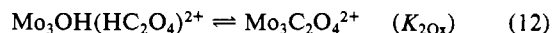
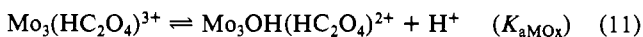
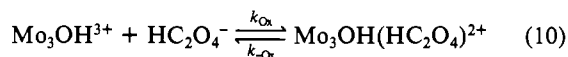
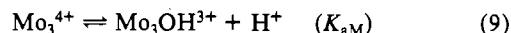
$$k'_{\text{eq}} = k'_f[\text{Ox}]_T/3 + k'_{\text{aq}} \quad (7)$$

were not large enough for runs to be carried out with the reactant $\text{Mo}_3\text{O}_4^{4+}$ present in large excess, and the statistical factor of 3 has been assumed to apply. Values of k'_f and k'_{aq} are given in Table IV.

For the range of $[\text{H}^+]$ values investigated, oxalate is present as $\text{H}_2\text{C}_2\text{O}_4$ and HC_2O_4^- . A value of the acid dissociation constant K_{aOx} , (8), of 0.084 M at 25 °C, $I = 1.0$ M (NaClO_4), has been



used.¹⁷ Other relevant reactions are as in (9)–(12). For the



(17) Denneux, M.; Meilleur, R.; Benoit, R. L. *Can. J. Chem.* **1968**, *46*, 1383. The value of K_{aOx} used was determined in 1.0 M NaClO_4 . From a comparison with literature values (e.g.: *Stability Constant Handbook*; Special Publication No. 17; Chemical Society: London, 1971), a realistic range of values to consider in the context of the present work is $K_{\text{aOx}} = 0.10$ M ($I = 0.5$ M, LiClO_4), giving $K_{\text{aM}} = 0.44$ M and $k_{\text{ox}} = 2.85 \text{ M}^{-1} \text{ s}^{-1}$, to $K_{\text{aOx}} = 0.055$ M ($I = 3.0$ M, NaClO_4), giving $K_{\text{aM}} = 0.48$ M and $K_{\text{Ox}} = 4.4 \text{ M}^{-1} \text{ s}^{-1}$.

(16) Alcock, N. W.; Denton, D. J.; Moore, P. *Trans. Faraday Soc.* **1970**, *6*, 2210.

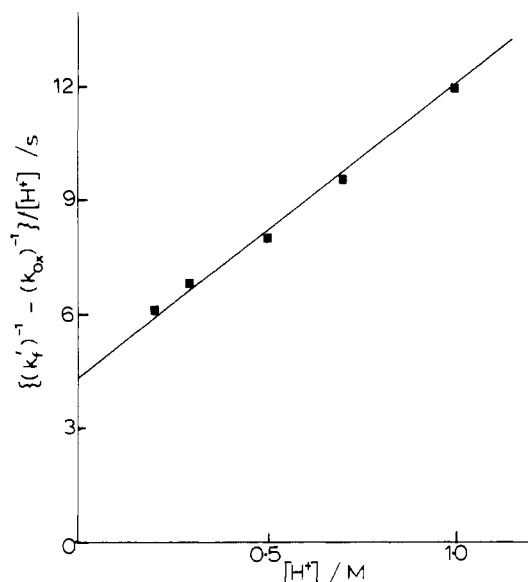


Figure 6. Plot illustrating the dependence of k'_f (25 °C), for the $\text{Mo}_3\text{O}_4^{4+}$ and oxalate complex formation step, on $[\text{H}^+]$, eq 14; $I = 2.00$ M (LiPTS).

formation process (13) is obtained. Values of $k'_f([\text{H}^+] + K_{aOx})([\text{H}^+] + K_{aM})$ are independent of $[\text{H}^+]$ (K_{aM} from the NCS⁻

$$k'_f = \frac{k_{Ox}K_{aOx}K_{aM}}{([\text{H}^+] + K_{aOx})([\text{H}^+] + K_{aM})} \quad (13)$$

study), consistent with (13), and there is no evidence for contributions from the reactions of Mo_3^{4+} with HC_2O_4^- . On rearrangement of (13), (14) is obtained. For estimates of k_{Ox} , a plot

$$\left(\frac{1}{k'_f} - \frac{1}{k_{Ox}}\right) \frac{1}{[\text{H}^+]} = \frac{[\text{H}^+]}{k_{Ox}K_{aOx}K_{aM}} + \frac{K_{aOx} + K_{aM}}{k_{Ox}K_{aOx}K_{aM}} \quad (14)$$

of the left-hand side against $[\text{H}^+]$ is linear (Figure 6). From the slope and intercept k_{Ox} can be refined (in an iterative manner), to give a best fit with $k_{Ox} = 3.3 \pm 0.9 \text{ M}^{-1} \text{ s}^{-1}$ and $K_{aM} = 0.45 \pm 0.09 \text{ M}$.

For the k'_{aq} process the corresponding $[\text{H}^+]$ dependence is as in (15), which can be rearranged to give (16). A graph of k'_{aq}^{-1}

$$k'_{aq} = \frac{k_{-Ox}K_{aMOx}K_{2Ox}[\text{H}^+]}{[\text{H}^+] + K_{aMOx}K_{2Ox}} \quad (15)$$

$$\frac{1}{k'_{aq}} = \frac{1}{k_{-Ox}K_{aMOx}K_{2Ox}} + \frac{1}{k_{-Ox}[\text{H}^+]} \quad (16)$$

against $[\text{H}^+]^{-1}$ (Figure 7) gives $k_{-Ox} = (1.10 \pm 0.06) \times 10^{-3} \text{ s}^{-1}$ and $K_{aMOx}K_{2Ox} = 1.51 \pm 0.46 \text{ M}$.

The $[\text{H}^+]$ dependence of equilibration rate constants for the chelation step, k_{chel} in Table III, is illustrated in Figure 8.

Discussion

The acid dissociation constants, K_{aM} , for the trimeric Mo(IV) aqua ion $[\text{Mo}_3\text{O}_4(\text{H}_2\text{O})_9]^{4+}$ has been determined for the first time. From independent kinetic substitution studies at 25 °C, $I = 2.00$ M (LiPTS), K_{aM} is 0.39 M (with NCS⁻) and 0.45 M (oxalate). The values obtained are larger than might have been anticipated for a Mo(IV) ion that is already bonded to three (bridging) oxo 2-ligands. At $[\text{H}^+] \sim 0.4 \text{ M}$ equal concentrations of trimer and conjugate base, Mo_3^{4+} and $\text{Mo}_3\text{OH}^{3+}$, are present. At this $[\text{H}^+]$ (and less), care is required therefore to limit oligomerization, and it is necessary to work with fresh solutions (from more concentrated $[\text{H}^+]$ stock solutions) and at low $[\text{Mo}_3\text{O}_4^{4+}]$. Present studies were restricted to a lower limit of $[\text{H}^+] = 0.20 \text{ M}$ and to $[\text{Mo}_3\text{O}_4^{4+}]$ generally $0.04 \times 10^{-3} \text{ M}$. For runs at $[\text{H}^+] = 0.20$ and 0.25 M , with $[\text{Mo}_3\text{O}_4^{4+}] \sim 0.5 \times 10^{-3} \text{ M}$ (reactant in excess), discrepancies attributable to oligomerization were observed with rate constants 8–10% higher.

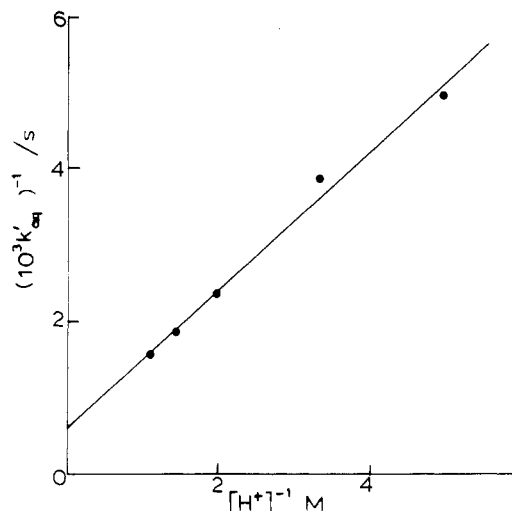


Figure 7. Plot illustrating the dependence of k'_{aq} (25 °C), for the aquation of the $\text{Mo}_3\text{O}_4^{4+}$ and oxalate monodentate complex, on $[\text{H}^+]$, eq 16; $I = 2.00$ M (LiPTS).

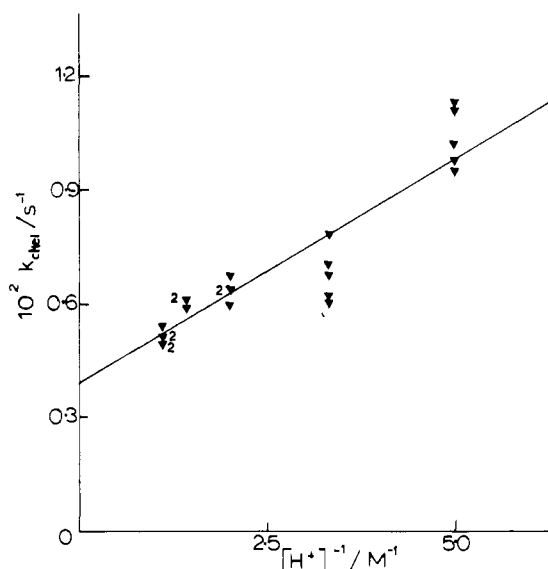


Figure 8. Variation of equilibration rate constants, k_{chel} (25 °C), for the chelation step in the complexation of $\text{Mo}_3\text{O}_4^{4+}$ and oxalate, with $[\text{H}^+]^{-1}$; $I = 2.00$ M (LiPTS).

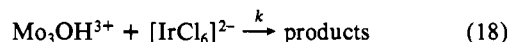
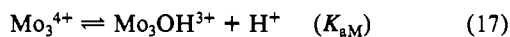
As far as we can tell, substitution reactions proceed solely by conjugate-base pathways. The similarity of k_{-T} ($4.8 \text{ M}^{-1} \text{ s}^{-1}$) and k_{Ox} ($3.3 \text{ M}^{-1} \text{ s}^{-1}$) is consistent with a dissociative interchange (I_d) mechanism. From crystallographic studies on $[\text{Mo}_3\text{O}_4(\text{C}_2\text{O}_4)_3(\text{H}_2\text{O})_3]^{2-}$, the $\text{C}_2\text{O}_4^{2-}$ ligands are coordinated to two d- H_2O positions.¹ The relevant conjugate base would be expected to form at the c- H_2O 's, which (a) are the more inert H_2O 's^{4,7} and (b) have shorter Mo–OH₂ bonds.^{1,3} This does not appear to be the case however from ¹⁷O NMR studies, which have demonstrated that only the d- H_2O 's, and not the c- H_2O 's, give detectable acid dissociation over the range $[\text{H}^+] = 0.1\text{--}1.0 \text{ M}$ at $I = 1.0 \text{ M}$.¹⁸ This result is difficult to explain¹⁸ but is assumed to be relevant to the present studies. Ultimately, in substitution reactions with a very large excess of NCS⁻ (much higher than used in the present studies), $[\text{Mo}_3\text{O}_4(\text{NCS})_9]^{5-}$ is formed,⁴ and for the last three or possibly six NCS⁻ complexation steps substitution must proceed by other than a conjugate-base pathway. Replacement of these H_2O 's could well be at a slower rate therefore. When oxalate reacts with aqua $\text{Mo}_3\text{O}_4^{4+}$, a two-stage process is observed, which we envisage as the formation of a species containing monodentate

(18) Helm, L.; Pittet, P. A.; Richens, D. T.; Merbach, A. E., to be submitted for publication.

oxalate HC_2O_4^- , followed by a faster step involving chelation (with displacement of a second H_2O). The three remaining H_2O 's of $[\text{Mo}_3\text{O}_4(\text{C}_2\text{O}_4)_3(\text{H}_2\text{O})_3]^{2-}$ are not readily replaced.⁴

The aquation of NCS^- and monodentate oxalate and chelation of monodentate HC_2O_4^- also proceed via conjugate-base paths. The acid dissociation constant (K_{aMT}) obtained for $[\text{Mo}_3\text{O}_4\text{NCS}(\text{H}_2\text{O})_8]^{3+}$ is 0.19 M and the presence of the adjacent negatively charged NCS^- ligands brings about a decrease as compared to K_{aM} (0.42 M). For the monodentate oxalato complex $[\text{Mo}_3\text{O}_4(\text{C}_2\text{O}_4\text{H})(\text{H}_2\text{O})_8]^{3+}$ the composite term $K_{\text{aMOx}}K_{2\text{Ox}} = 1.51$ M is obtained, which cannot be compared directly with K_{aMT} . In this case, acid dissociation of the monodentate $\text{C}_2\text{O}_4\text{H}^-$ most likely gives the $[\text{H}^+]$ dependence in Figure 8. If this is the case, then the reverse step in (12) corresponding to addition of H_2O will be independent of $[\text{H}^+]$.

In an earlier study¹³ of the $[\text{IrCl}_6]^{2-}$ oxidation of $\text{Mo}_3\text{O}_4^{4+}$ in 2 M H^+/Li^+ perchlorate (which indicated a rate law first order in both $[\text{IrCl}_6^{2-}]$ and $[\text{Mo}_3\text{O}_4^{4+}]$ (giving second-order rate constants k_{Ir})), it was possible to assign an inner-sphere mechanism. A dominant inverse $[\text{H}^+]$ dependence was reported. We are now able to reformulate the reaction as in (17) and (18). At 25 °C



with the exclusion of the two points at lower $[\text{H}^+]$ (solutions of $\text{Mo}_3\text{O}_4^{4+}$ in ClO_4^- are less stable under these conditions), a satisfactory linear plot of k_{Ir}^{-1} against $(K_{\text{a}} + [\text{H}^+])$ is obtained by using $K_{\text{aM}} = 0.42$ M (average value as determined above). This plot gives $k = 4.5 \text{ M}^{-1} \text{ s}^{-1}$, in very good agreement with k_{NCS} ($4.8 \text{ M}^{-1} \text{ s}^{-1}$) and k_{Ox} ($3.3 \text{ M}^{-1} \text{ s}^{-1}$). It appears therefore that the $[\text{IrCl}_6]^{2-}$ reaction is inner sphere and could well be substitution controlled.

The dominance of a conjugate-base I_d mechanism for substitution is of interest, because low-d-electron-population mononuclear hexaaqua ions, such as $\text{Ti}(\text{III})(3d^1)$,¹⁹ $\text{V}(\text{III})(3d^2)$,²⁰ and

(19) Hugi, A. D.; Helm, L.; Merbach, A. E. *Inorg. Chem.* 1987, 26, 1763.

$\text{Mo}(\text{III})(4d^3)$,^{21,22} are known to react by an associative interchange (I_a) process. For $\text{Mo}(\text{IV})(4d^2)$ in $\text{Mo}_3\text{O}_4^{4+}$ metal-metal bonding results in pseudo-eight-coordination at each Mo, and crowding of the Mo site appears to exclude an I_a process. Existing evidence suggests that substitution reactions involving conjugate-base forms proceed by an I_d mechanism.²³

In the present studies we have no information as to the extent of ion-pair formation preceding the replacement of H_2O by NCS^- , HC_2O_4^- , or $[\text{IrCl}_6]^{2-}$. The similarity of the $[\text{IrCl}_6]^{2-}$ data suggests that there are no large differences between 1- and 2- reactants. Ion pairing is likely to be at the aqua ligand face on each $\text{Mo}(\text{IV})$, thus avoiding interactions with negatively charged μ -oxo core ligands. The effective positive charge on each $\text{Mo}(\text{IV})$ at 1.33 is small.

Finally, it is of interest that UV-vis absorbance changes corresponding to the formation of the conjugate base of $\text{Mo}_3\text{O}_4^{4+}$ are small in solutions containing HPTS, which itself absorbs strongly below 300 nm. Even at $[\text{H}^+] \sim 0.42$ M, when $[\text{Mo}_3^{4+}]$ and $[\text{Mo}_3\text{OH}^{3+}]$ are equal, changes in the UV-vis absorbance spectrum are barely detectable above 300 nm. Similarly, it is extremely difficult distinguishing between the chloro complexes $\text{Mo}_3\text{O}_4\text{Cl}^{3+}$ and $\text{Mo}_3\text{O}_4\text{Cl}_2^{2+}$ and aqua $\text{Mo}_3\text{O}_4^{4+}$ from UV-vis spectra. Substitution at external (c and d) coordination sites has only a very mild effect on absorbance of the $\text{Mo}_3\text{O}_4^{4+}$ core. Oxalate and thiocyanate, which give charge-transfer contributions, are somewhat unusual therefore in this context.

Acknowledgment. We are grateful to the University of Newcastle upon Tyne for a Ridley Fellowship (to B.-L.O.) and thank Professor André Merbach and colleagues in Lausanne for information¹⁸ prior to publication.

Registry No. $[\text{Mo}_3\text{O}_4(\text{H}_2\text{O})_9]^{4+}$, 108772-69-6; NCS^- , 302-04-5; HC_2O_4^- , 920-52-5.

(20) Hugi, A. D.; Helm, A.; Merbach, A. E. *Helv. Chim. Acta* 1985, 68, 508.

(21) Sasaki, Y.; Sykes, A. G. *J. Chem. Soc., Dalton Trans.* 1975, 1048.

(22) Richens, D. T.; Ducommun, Y.; Merbach, A. E. *J. Am. Chem. Soc.* 1987, 109, 603.

(23) Swaddle, T. W.; Merbach, A. E. *Inorg. Chem.* 1981, 20, 4212.

Contribution from the Ames Laboratory and Department of Chemistry, Iowa State University, Ames, Iowa 50011

Reductive Quenching of ${}^2\text{E Cr}(\text{bpy})_3^{3+}$ by Fe^{2+} and $\text{Cr}(\text{bpy})_3^{2+}$

Andreja Bakac,* Khurram Zahir, and James H. Espenson*

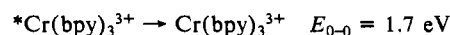
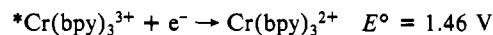
Received November 4, 1987

The reductive quenching of the doublet excited state of $\text{Cr}(\text{bpy})_3^{3+}$ by $\text{Fe}(\text{H}_2\text{O})_6^{2+}$ at pH 1 in aqueous perchlorate solutions produces $\text{Cr}(\text{bpy})_3^{2+}$; $k = (5.3 \pm 0.3) \times 10^6 \text{ M}^{-1} \text{ s}^{-1}$ at 25 °C and 1 M ionic strength. Concurrent reduction of ${}^2\text{E Cr}(\text{bpy})_3^{3+}$ by $\text{Cr}(\text{bpy})_3^{2+}$, unrecognized in previous studies, provides a catalytic route for the deactivation of the excited state. This reaction can be eliminated by the addition of $\text{Fe}(\text{H}_2\text{O})_6^{2+}$, which rapidly oxidizes the chromium(II) complex; $k = 9.2 \times 10^8 \text{ M}^{-1} \text{ s}^{-1}$. The quenching of ${}^2\text{E Cr}(\text{bpy})_3^{3+}$ by $\text{Cr}(\text{bpy})_3^{2+}$ was demonstrated by the effect of Fe^{2+} on the excited state lifetimes and yields of $\text{Cr}(\text{bpy})_3^{2+}$ in experiments with Fe^{2+} as quencher. This required solution of the differential rate equations by numerical integration; the program KINSIM was used and gave the value $k_{\text{Cr}} = (5 \pm 3) \times 10^9 \text{ M}^{-1} \text{ s}^{-1}$. The indicated quenching reaction was also observed directly.

Introduction

The high reduction potential^{1,2} and long lifetime ($\sim 70 \mu\text{s}$)¹⁻³ of ${}^2\text{E Cr}(\text{bpy})_3^{3+}$, denoted ${}^*\text{Cr}(\text{bpy})_3^{3+}$, as well as its reactivity in energy-transfer reactions,⁴⁻⁸ have made ${}^*\text{Cr}(\text{bpy})_3^{3+}$ one of the

most intensely studied metal-centered excited states in the past decade.



Of all the electron-transfer reactions of ${}^*\text{Cr}(\text{bpy})_3^{3+}$ reported to date, that with Fe^{2+} has received the most attention. The initial

(1) Balzani, V.; Bolletta, F.; Gandolfi, M. T.; Maestri, M. *Top. Curr. Chem.* 1978, 75, 1.

(2) Jamieson, M. A.; Serpone, N.; Hoffman, M. Z. *Coord. Chem. Rev.* 1981, 39, 121.

(3) Maestri, M.; Bolletta, F.; Moggi, L.; Balzani, V.; Henry, M. S.; Hoffman, M. Z. *J. Am. Chem. Soc.* 1978, 100, 2694.

(4) Juris, A.; Manfrin, M. F.; Maestri, M.; Serpone, N. *Inorg. Chem.* 1978, 17, 2258.

(5) Gandolfi, M. T.; Maestri, M.; Sandrini, D.; Balzani, V. *Inorg. Chem.* 1983, 22, 3435.

(6) Endicott, J. F.; Ramasami, T.; Gaswick, D. C.; Tamilarasan, R.; Heeg, M. J.; Brubaker, G. R.; Pyke, S. C. *J. Am. Chem. Soc.* 1983, 105, 5301.

(7) Bolletta, F.; Maestri, M.; Balzani, V. *J. Phys. Chem.* 1976, 80, 2499.

(8) Endicott, J. F.; Heeg, M. J.; Gaswick, D. C.; Pyke, S. C. *J. Phys. Chem.* 1981, 85, 1777.